



# ***Porphyromonas gingivalis*-induced inflammatory responses in THP1 cells are altered by native and modified low-density lipoproteins in a strain-dependent manner**

KARTHEYAENE JAYAPRAKASH,\* ISAK DEMIREL,\* HAZEM KHALAF and TORBJÖRN BENGTTSSON

Department of Medical Sciences, Örebro University, Örebro, Sweden

Jayaprakash K, Demirel I, Khalaf H, Bengtsson T. *Porphyromonas gingivalis*-induced inflammatory responses in THP1 cells are altered by native and modified low-density lipoproteins in a strain-dependent manner. APMIS 2018; 126: 667–677.

Strong epidemiological evidence supports an association between cardiovascular and periodontal disease and furthermore, the periodontopathogen *Porphyromonas gingivalis* has been identified in blood and from atheromatous plaques. Blood exposed to *P. gingivalis* shows an increased protein modification of low-density lipoprotein (LDL). In this study, we investigate the inflammatory responses of THP1 cells incubated with *P. gingivalis* and the effects of native or modified LDL on these responses. Reactive oxygen species (ROS) and IL-1 $\beta$  were observed in THP1 cells following infection with *P. gingivalis* ATCC33277 and W50. Caspase 1 activity was quantified in THP1 cells and correlated with IL-1 $\beta$  accumulation. Oxidized LDL (oxLDL) induced IL-1 $\beta$  release and CD36 expression on THP1 cells. Modified LDL co-stimulated with ATCC33277 exhibited regulatory effects on caspase 1 activity, IL-1 $\beta$  release and CD36 expression in THP1 cells, whereas W50 induced more modest responses in THP1 cells. In summary, we show that *P. gingivalis* is capable of inducing pro-inflammatory responses in THP1 cells, and native and modified LDL could alter these responses in a dose- and strain-dependent manner. Strain-dependent differences in THP1 cell responses could be due to the effect of *P. gingivalis* proteases, presence or absence of capsule and proteolytic transformation of native and modified LDL.

Key words: Periodontitis; caspase 1; CD36; inflammation; IL-1beta.

Kartheyaene Jayaprakash, Department of Medical Sciences, Örebro University, Fakultetsgatan 1, 70182, Örebro, Sweden. e-mail: kartheyaene.jayaprakash@oru.se

\*Contributed equally.

The periodontal diseases reflect a spectrum of oral pathology from gingivitis to severe periodontitis with alveolar bone and tooth loss due to accumulation of predominantly gram-negative subgingival bacterial biofilms, with consequent mucosal inflammation (1). Foremost among this bacterial biofilms are three species, which comprise the so-called “red complex”, a pathogenic consortium in periodontitis: *Porphyromonas gingivalis* (*P. gingivalis*), *Treponema denticola*, and *Tannerella forsythia* (2). *Porphyromonas gingivalis* is a gram-negative anaerobic,

proteolytic species of bacteria strongly associated with the etiology of periodontitis and also known as a ‘keystone pathogen’. In combination with other oral anaerobes, *P. gingivalis* has been shown to degrade immunoglobulin, inhibit the complement system and produce toxic components such as lipopolysaccharide (LPS) and gingipains. These factors sustain bacterial viability during bacteremia, which commonly occurs as a result of surgical treatments, tooth brushing, and other dental procedures (3, 4).

The innate immune response to transient bacteremia and the direct involvement of inflammatory

mediators activated by dental plaque, are common predisposing factors which influence both periodontitis and atherosclerosis. Mounting evidence over the last two decades, substantiate an association between dental plaque bacteria and atherosclerotic coronary diseases, inferring periodontitis as a new aspect to the etiology of atherosclerosis (5–7). However, lack of causative evidence suggests that it is time to enter the next phase of research by conducting studies at the cellular and molecular level. These studies should be appropriately designed to test our current understanding of the involved molecular mechanisms (8).

Low-density lipoprotein (LDL) transports cholesterol and triglycerides to cells, via the circulation. However, LDL also plays an important role in the development of atherosclerotic cardiovascular diseases. The major protein component of native LDL is apolipoprotein B-100 (apo B-100) (9). Studies have indicated that infection and inflammation are associated with an increase in small dense LDL, which is believed to be more pro-atherogenic because of its longevity in circulation, avid affinity to intra-arterial proteoglycans and increased susceptibility to oxidation. This modified LDL causes an enhanced uptake by macrophages (10, 11).

LDL isolated from patients with periodontal disease enhances the uptake of cholesterol esters by macrophages (12). We have shown that exposing human blood to *P. gingivalis* and its gingipains leads to protein modification, including elevated levels of apoM and formation of two apo B-100 N-terminal fragments (13). However, the knowledge of the interaction between *P. gingivalis* and LDL is currently limited and needs to be further elucidated. *Porphyromonas gingivalis* produces several types of proteolytic enzymes that can modify LDL, including gingipains, collagenases, dipeptidyl aminopeptidase IV, and peptidyl arginyl deiminase enzymes, which are very crucial for its virulence and colonization. *Porphyromonas gingivalis* gingipains are trypsin-like cysteine proteinases-Arginine (RgpA/B) and Lysine (Kgp) gingipains. ATCC33277 and W50 are wild-type *P. gingivalis* strains that express RgpA/B and Kgp. Furthermore, *P. gingivalis*-modified LDL has been shown to be a potent inducer of macrophage foam cell formation (13–15).

In the process of oxidation and proteolytic modification, the apo B in LDL is changed, which increases the affinity to scavenger receptors, such as CD36 and lectin-like oxidized low-density lipoprotein receptor-1 (16). Scavenger receptors are present on macrophages in atherosclerotic lesions and play a critical role in foam cell formation because of their ability to bind modified LDL, such as oxidized LDL (oxLDL) and acetylated LDL. They

function by transporting lipids and cholesterol into and out of the cells. CD36 is a lipid raft-associated glycosylated protein present on platelets, mononuclear phagocytes, adipocytes, hepatocytes, myocytes, and some epithelia. Various ligands, such as oxLDL, apoptotic cells, and advanced glycated end products bind to this receptor. CD36 participates in the internalization of apoptotic cells, certain bacterial and fungal pathogens, and modified LDL, thus contributing to inflammatory responses and atherothrombotic diseases (17, 18). CD36 liaises with toll-like receptor 2 (TLR2) or TLR heterodimer TLR4-TLR6 to recognize *P. gingivalis* and oxLDL. This induces inflammatory responses such as activation of the transcription factor nuclear factor  $\kappa$ B (NF- $\kappa$ B), release of Interleukin-1 $\beta$  (IL-1 $\beta$ ), and production of reactive oxygen species (ROS) (18–21).

Besides, CD36 cooperates with TLR4-TLR6 to prime the inflammasome, which is a large, multi-protein complex, in which pro-caspase 1 is cleaved into mature caspase 1. Activated caspase 1 is capable of cleaving pro-IL-1 $\beta$  into its bioactive form IL-1 $\beta$ , which has been linked to the pathogenesis of several sterile inflammatory diseases, including atherosclerosis, type 2 diabetes, and Alzheimer's disease (22, 23). This entails that CD36 is a critical sensor of metabolic and pathogenic stresses in vascular inflammation.

Most studies have addressed the effects of CD36, and oxLDL induced foam cell formation in macrophages. However, a recent study confirmed that foamy monocytes were formed early and contributed to initial stages of atherosclerosis in mice with hypercholesterolemia (24). We hypothesized that *P. gingivalis*-induced inflammatory responses, in the monocyte surrogate THP1 cell line, could be regulated by native and modified LDL. In this study, we investigate the inflammatory responses of THP1 cells incubated with *P. gingivalis* and the effects of native or modified LDL on these responses.

## METHODS

### Cell culture

THP1 (TIB-202, American Type culture collection, Manassas, VA, USA) cells were grown in RPMI-1640 containing 10% fetal bovine serum (FBS) at 37 °C and 5% CO<sub>2</sub>. The logarithmic growth of the cells was maintained between  $2 \times 10^5$  to  $1 \times 10^6$  cells/mL by passage, every 3–4 days. A cell concentration of  $1 \times 10^6$  cells/mL per well was used in a six-well plate during each experiment in RPMI-1640 containing 10% FBS.

### Bacterial culture and preparation

*Porphyromonas gingivalis* ATCC33277 (American Type Culture Collection, Manassas, VA, USA) and *P. gingivalis* W50 (a kind gift from Dr. M. Curtis, Barts and The London, Queen Mary's School of Medicine and Dentistry, London, UK), were grown in fastidious anaerobic broth (Lab M Limited, Lancashire, UK). The bacteria were cultured for 72 h in an anaerobic chamber (Concept 400 Anaerobic Workstation; Ruskinn Technology Ltd., Leeds, UK), containing 80% N<sub>2</sub>, 10% CO<sub>2</sub>, and 10% H<sub>2</sub> at 37 °C. The bacteria were centrifuged at 9300 g for 10 min at room temperature, washed twice with Krebs- Ringer glucose buffer (KRG) free of calcium (120 mM NaCl, 4.9 mM KCl, 1.2 mM MgSO<sub>4</sub>, 1.7 mM KH<sub>2</sub>PO<sub>4</sub>, 8.3 mM Na<sub>2</sub>HPO<sub>4</sub>, and 10 mM glucose, pH 7.3) and resuspended in fresh KRG buffer without calcium and the concentration was adjusted to 1 × 10<sup>9</sup> CFU/mL. Thirty microliters of each serial diluted bacterial suspension was plated on fastidious anaerobic agar (Acumedia, Neogen, Lansing, MI, USA) plate enriched with 5% defibrinated horse blood and incubated for 7 days in the anaerobic chamber for a subsequent colony count. In order to stimulate the THP1 cells, MOI (multiplicity of infection) 100, 10 or 1, live bacteria, was used and incubated between 30 min up to 6 h in a stable environment of 37 °C, 5% CO<sub>2</sub> and 95% air.

### Low-density lipoproteins

Human LDL (LDL; BT-903) and Oxidized LDL (oxLDL; BT-910) (Hycultec, Beutelsbach, Germany) were diluted in PBS. The oxLDL used in this study is a copper sulfate oxidized (moderately oxidized) variant. THP1 cells were incubated with 60 µg/mL LDL or oxLDL with or without MOI100, MOI10 or MOI1 ATCC33277 or W50. In some experiments, LDL was co-incubated with live *P. gingivalis* ATCC33277 or W50 for 30 min prior to stimulation of THP1 cells. This is further referred to as pre-incubated LDL or simply 'pLDL'.

### Measurement of ROS production

The production of ROS by THP1 cells was measured by using luminol-dependent chemiluminescence assay. Luminol is excited by ROS and the evoked chemiluminescence is proportional to ROS production. THP1 cells in RPMI-1640 containing 10% FBS were incubated with luminol (0.1 mg/mL, Sigma-aldrich, St.Louis, Missouri, USA) and horseradish peroxidase (HRP; 4 U/mL, Roche, Basel, Switzerland) for 15 min at 37 °C in a 96-well plate.

THP1 cells were stimulated with MOI100, 10 or 1 live ATCC33277 or W50 with or without LDL. Untreated THP1 cells serve as the negative control. The plate was centrifuged at 400 g at 4 °C for 3 min and the chemiluminescence was measured in a microplate reader (Fluostar Optima, BMG Labtech, Aylesbury, UK) at 37 °C every third minute for 6 h. All samples were run in duplicate.

### Caspase 1 assay

THP1 cells were seeded at a concentration of 1 × 10<sup>6</sup> cells/mL in a 96-well plate. Cells were treated with solvent control Dimethyl sulfoxide (DMSO) or with 50 µM Ac-YVAD-AMC (Enzo Life Sciences, New York, NY, USA) for 1 h at 37 °C and 5% CO<sub>2</sub>. Following which, the cells were stimulated with MOI100, 10 or 1 live ATCC33277 or W50 with or without LDL. The plate was read after 30 min, 1, 2, 4, and 6 h in a fluorescent plate reader (Fluostar Optima, Ortenberg, Germany) at excitation/emission 340/440 nm.

### ELISA analysis of IL-1β

Enzyme-linked immunosorbent assay (ELISA) was performed on culture supernatant of THP1 cells incubated with the different strains of live *P. gingivalis* with or without LDL to measure IL-1β. After co-incubations for 30 min, 1, 2, 4, and 6 h, the cell culture suspension was centrifuged at 1200 g for 5 min at room temperature and the cell-free supernatants were aliquoted and stored at -80 °C until further analysis using Human IL-1β ELISA kit (Biolegend, Sandiego, CA, USA).

### Scanning confocal laser microscopy

THP1 cells were infected with MOI100 live ATCC33277 or W50, in the presence or absence of LDL, oxLDL or with pLDL in an eight-well chamber slide (Sarstedt, Germany) for 6 h. Following the incubation, the wells were washed gently with PBS, pH 7.2. The samples were fixed with ice-cold 4% paraformaldehyde for 40 min at room temperature and then washed gently with PBS. Following this, the cells were incubated in ice-cold PBS containing 0.1% Triton-×100 for 10 min. The cells were washed gently with ice-cold PBS followed by blocking in 1% BSA in PBS containing 0.1% Triton-×100 for 30 min at room temperature. The cells were again washed with ice-cold PBS and incubated with 1:200 FITC-conjugated CD36 rabbit polyclonal antibody (Novus Biologicals, Littleton, CO, USA) in ice-cold PBS for 1 hour. The cells were washed again and stained for F-actin using

Rhodamine phalloidin (5U/200  $\mu$ l, Life Technologies, Carlsbad, California, USA) for 20 min in the dark. The wells were washed twice with PBS and the nucleus was stained using 4', 6'-diamidino-2-phenylindole hydrochloride (DAPI, Sigma) 5 min in the dark and washed with PBS. ProLong<sup>®</sup> Gold antifade reagent (Invitrogen) was added to the samples which were stored in the dark at 4 °C until viewed under the microscope. The images were obtained under oil immersion at 60 $\times$  magnification by confocal laser scanning microscopy (Olympus Fluoview, Hamburg, Germany) and processed with the Fluoview 10 ASW 2.0 software (Mississauga, ON, Canada). The representative image for each condition was scanned and fluorescence was quantified using ImageJ and expressed as mean fluorescence intensity (MFI = Total image fluorescence/ Number of cells in the image) (25).

**Statistical analysis**

The statistically significant differences of data between groups and over time, were assessed using two-way ANOVA with Bonferroni post-hoc corrections. All data were analyzed using GraphPad Prism5 (GraphPad software, La Jolla, CA, USA) and are represented as mean values with standard deviation (SD). p-Value < 0.05 was considered significant.

**RESULTS**

***Porphyromonas gingivalis* infection results in ROS production, caspase 1 activation, and IL-1 $\beta$  release from THP1 cells**

We have quantified ROS in THP1 cells in response to infection with MOI1, 10 or 100 ATCC33277 (Fig. 1A) or W50 (Fig. 1D) after 30 min, 1, 2, 4, and 6 h. We show that MOI100 ATCC33277 induced rapid and significant ROS production that reached its peak at around 30 min followed by a gradual decrease. However at MOI10, we observed a modest increase in ROS, in comparison to MOI100 and these levels were maintained steady throughout. It is very clear that the amount of ROS induced by *P. gingivalis* ATCC33277 is dose-dependent. In W50-infected THP1 cells, MOI100 and MOI1 induced a similar pattern of ROS as observed in ATCC33277-infected cells. However, MOI10 W50-infected cells exhibited a slow but steady increase that increases significantly and exponentially around 2 h and continued to rise as opposed to MOI 100 that reached a peak at around 30 min and showed a decline after that.

Caspase 1 activation was observed at 30 min in MOI100 ATCC33277 (Fig. 1B) and W50 (Fig. 1E)-stimulated THP1 cells and continued to rise reaching a maximal level after 2 h. Similar pattern but lower values, were obtained at MOI10. MOI1

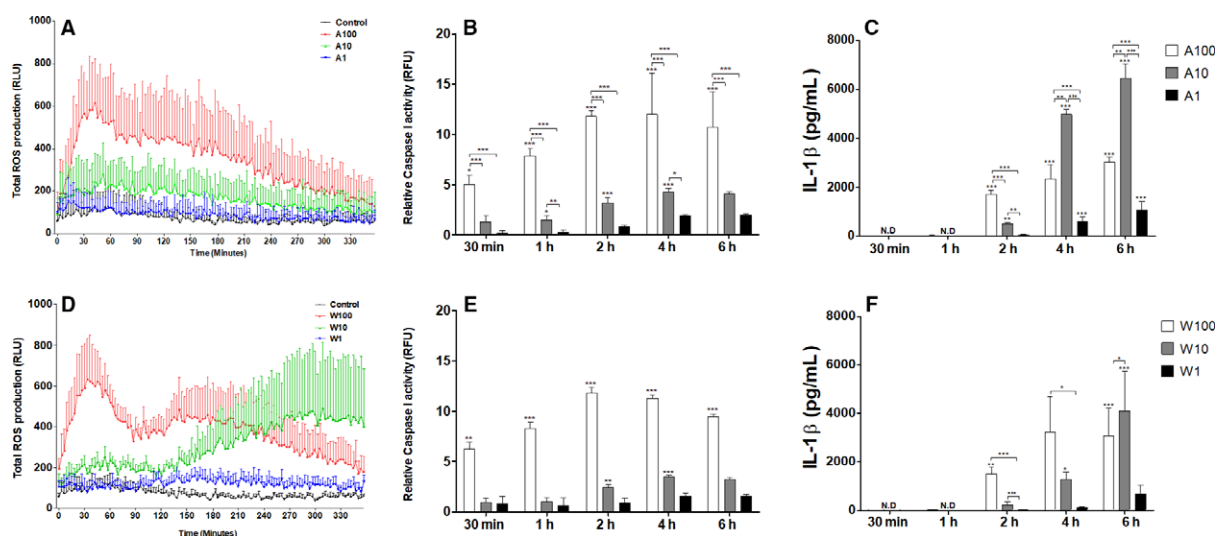


**Fig. 1.** *Porphyromonas gingivalis* induces ROS, caspase 1 activation and IL-1 $\beta$  release in THP1 cells. THP1 cells were stimulated with MOI100, MOI10, and MOI1 of *P. gingivalis* ATCC33277 or W50 for 30 min, 1, 2, 4, and 6 h. (A) ROS, (B) Caspase 1 activation and (C) IL-1 $\beta$  quantification from THP1 cells in response to ATCC33277 infection, (D) ROS, (E) Caspase 1 activation and (F) IL-1 $\beta$  quantification from THP1 cells in response to W50 infection. ROS (A and D) and IL-1 $\beta$  (C and F) were not detected at the various time points, in the untreated controls and hence not shown in the figures. Values represent the mean  $\pm$  SD. Statistically significant difference were determined using two-way ANOVA. (\*p < 0.05; \*\*p < 0.01; \*\*\*p < 0.001; n = 4). \* Placed right above the bars indicate significant differences in relation to the unstimulated control.

ATCC33277 showed a small but not significant increase in caspase 1 activation over time. W50-induced caspase 1 activation in THP1 cells was very similar to the effects of ATCC33277.

The IL-1 $\beta$  secretion was observed 2 h post-infection of THP1 cells by both MOI10 and MOI100 ATCC33277 (Fig. 1C) and W50 (Fig. 1F). Interestingly, at 4 and 6 h, the IL-1 $\beta$  concentration in supernatants of MOI10 ATCC33277-stimulated cells was higher than the amount of IL-1 $\beta$  released from MOI100-infected THP1 cells. In this manner, MOI10 W50-stimulated THP1 cells recorded a higher release of IL-1 $\beta$  at 6 h, compared to MOI100 W50-infected cells.

#### oxLDL induces CD36 expression and IL-1 $\beta$ release from THP1 cells

The ability of oxLDL to induce CD36 in THP1 cells was evident, as the untreated control and cells stimulated with native LDL show no or minimal CD36 expression (Fig. 2A–C). Almost all THP1 cells stimulated with oxLDL were positive for CD36 receptors with a mean average cellular

fluorescence intensity of ~8000 fluorescence units. In addition, oxLDL induced release of IL-1 $\beta$  from THP1 cells, whereas there was no IL-1 $\beta$  detected from cells incubated with native LDL (Fig. 2D).

#### The effects of LDL on *P. gingivalis*-induced IL-1 $\beta$ release from THP1 cells

We assessed the modulation of THP1 responses to *P. gingivalis* by co-stimulating MOI100, MOI10, or MOI1 *P. gingivalis* with 60  $\mu$ g/mL of native LDL, oxLDL, or pLDL. Upon quantifying IL-1 $\beta$  release, we found that native and modified LDL could significantly alter IL-1 $\beta$  release and accumulation by THP1 cells co-stimulated with ATCC33277, but not W50 (Fig. 3). Native LDL co-stimulated with ATCC33277 at MOI10, but not MOI100 or 1 induced significantly higher IL-1 $\beta$  release compared to ATCC33277 alone (Fig. 3). Furthermore, oxLDL co-stimulated with ATCC33277 at MOI100 and 10, but not MOI1 induced significantly higher IL-1 $\beta$  release compared to ATCC33277 alone (Fig. 3). This increase was synergistic rather than additive, as oxLDL by itself induced a modest IL-1 $\beta$  production

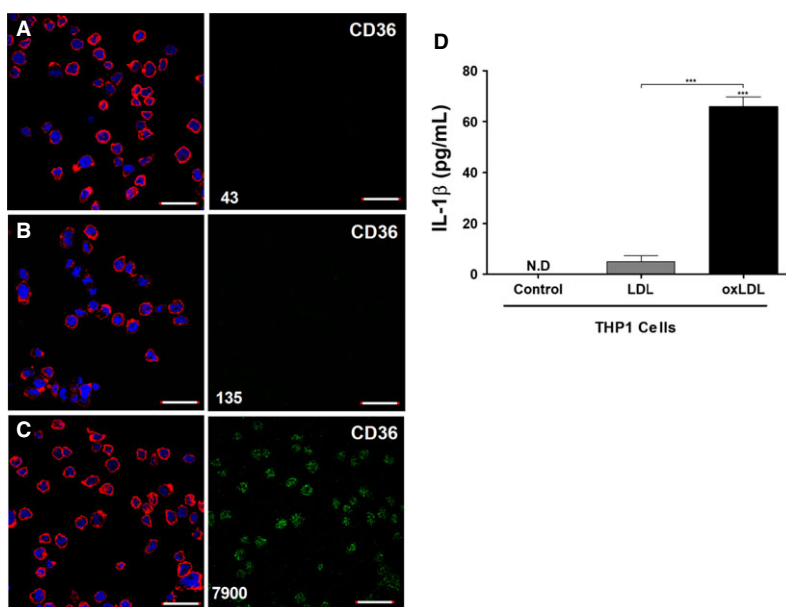


**Fig. 2.** THP1 cells express CD36 and secrete IL-1 $\beta$  in response to oxLDL. THP1 cells were: Unstimulated (A) or stimulated with 60  $\mu$ g/mL native LDL, (B) or 60  $\mu$ g/mL oxLDL and (C) for 6 h. FITC-labeled CD36 was added at 1:200 dilution and cells were further stained for actin with Rhodamine phalloidin (red) and nucleus with DAPI (blue). oxLDL stimulated THP1 cells were positive for CD36 expression shown with confocal fluorescence microscopy. Bar = 40  $\mu$ m. 60 $\times$  objective, oil immersion. Representative images from three independent experiments are shown. The representative image for each condition was scanned and fluorescence was quantified using ImageJ. Mean fluorescence intensity is indicated as numbers in the respective figures. IL-1 $\beta$  release was quantified at 6 h by THP1 cells in response to LDL (60  $\mu$ g/mL) and oxLDL (60  $\mu$ g/mL). Values represent the mean  $\pm$  SD. Statistically significant differences were determined using two-way ANOVA. (\* $p$  < 0.05; \*\* $p$  < 0.01; \*\*\* $p$  < 0.001;  $n$  = 3). \*Placed right above the bars indicate significant differences in relation to the control.

(Fig. 2D). In addition, we found that pLDL co-stimulated with ATCC33277 at MOI100 induced significantly lower IL-1 $\beta$  release compared to ATCC33277 alone or ATCC33277 co-stimulated with LDL. However, pLDL co-stimulated with ATCC 33277 at MOI1 induced significantly higher IL-1 $\beta$  release compared to ATCC33277 alone (Fig. 3C).

**The effects of LDL on *P. gingivalis*-induced caspase 1 activity in THP1 cells**

We continued with analyzing the effects of native LDL and modified LDL on *P. gingivalis*-induced caspase 1 activation in THP1 cells. Henceforth, we chose to analyze caspase 1 activity with MOI100 *P. gingivalis* ATCC33277 (Fig. 4A) or W50 (Fig. 4B). We found that native LDL co-stimulated

with ATCC33277 induced a significantly lower caspase 1 activation compared to ATCC33277 alone after 30 min. In addition, we also found that pLDL co-stimulated with ATCC33277 induced a significantly lower caspase 1 activation compared to ATCC33277 alone after 4 and 6 h. No significant difference was observed for oxLDL. Furthermore, W50-stimulated cells showed no alteration in caspase 1 activation in the presence of native or modified LDL as opposed to bacteria alone (Fig. 4B).

**LDL modulates *P. gingivalis*-induced CD36 expression in THP1 cells**

We show that both *P. gingivalis* and LDL were able to induce CD36 expression in THP1 cells (Fig. 5) and most specifically, oxLDL enhanced

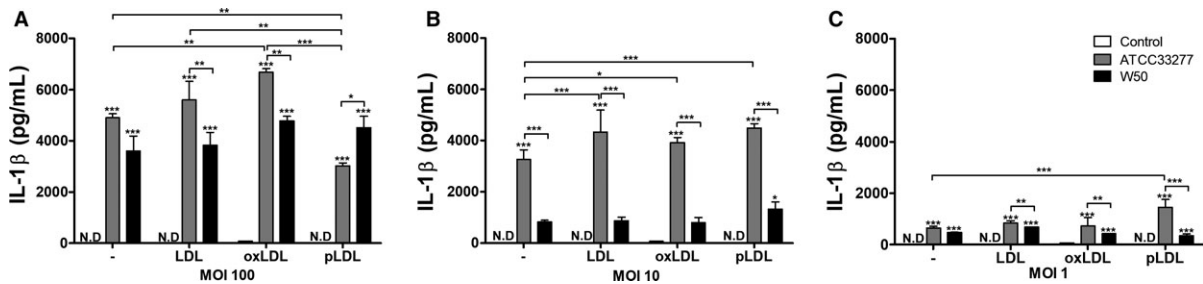


**Fig. 3.** The effects of different forms of LDL on *P. gingivalis*-induced IL-1 $\beta$  from THP1 cells. LDL was co-incubated with *P. gingivalis* ATCC33277 or W50, 30 min prior to stimulation of THP1 cells. This is referred to as pre-incubated LDL or simply 'pLDL'. THP1 cells were stimulated with LDL (60  $\mu$ g/mL), oxLDL (60  $\mu$ g/mL) or pLDL (60  $\mu$ g/mL), in the presence or absence of MOI100 (A) MOI10, (B) MOI1, and (C) *P. gingivalis* ATCC33277 or W50 for up to 6 h. IL-1 $\beta$  release from THP1 cells in response to ATCC33277 or W50 infection was quantified. Values represent the mean  $\pm$  SD. Statistically significant differences were determined using two-way ANOVA. (\* $p < 0.05$ ; \*\* $p < 0.01$ ; \*\*\* $p < 0.001$ ;  $n = 3$ ). \*Placed right above the bars indicate significant differences in relation to the respective control.

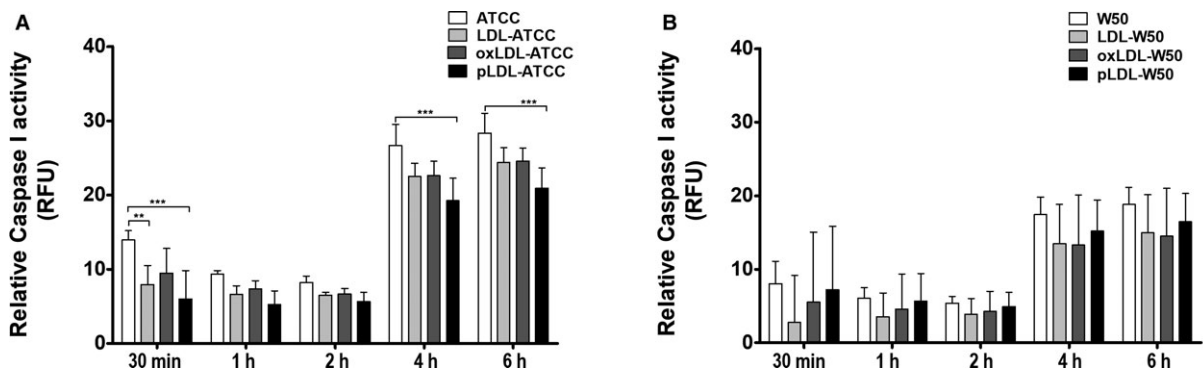


**Fig. 4.** The effects of different forms of LDL on *P. gingivalis*-induced caspase 1 in THP1 cells. LDL was co-incubated with *P. gingivalis* ATCC33277 or W50, 30 min prior to stimulation of THP1 cells. This is referred to as pre-incubated LDL or simply 'pLDL'. THP1 cells were stimulated with LDL (60  $\mu$ g/mL), oxLDL (60  $\mu$ g/mL) or pLDL (60  $\mu$ g/mL), in the presence or absence of MOI100 *P. gingivalis* ATCC33277 or W50 for up to 6 h and caspase 1 activity from THP1 cells in response to ATCC33277 (A) or W50 (B) infection was quantified. Values represent the mean  $\pm$  SD. Statistically significant differences were determined using two-way ANOVA. (\* $p < 0.05$ ; \*\* $p < 0.01$ ; \*\*\* $p < 0.001$ ;  $n = 3$ ). \*Placed right above the bars indicate significant differences in relation to the respective control.

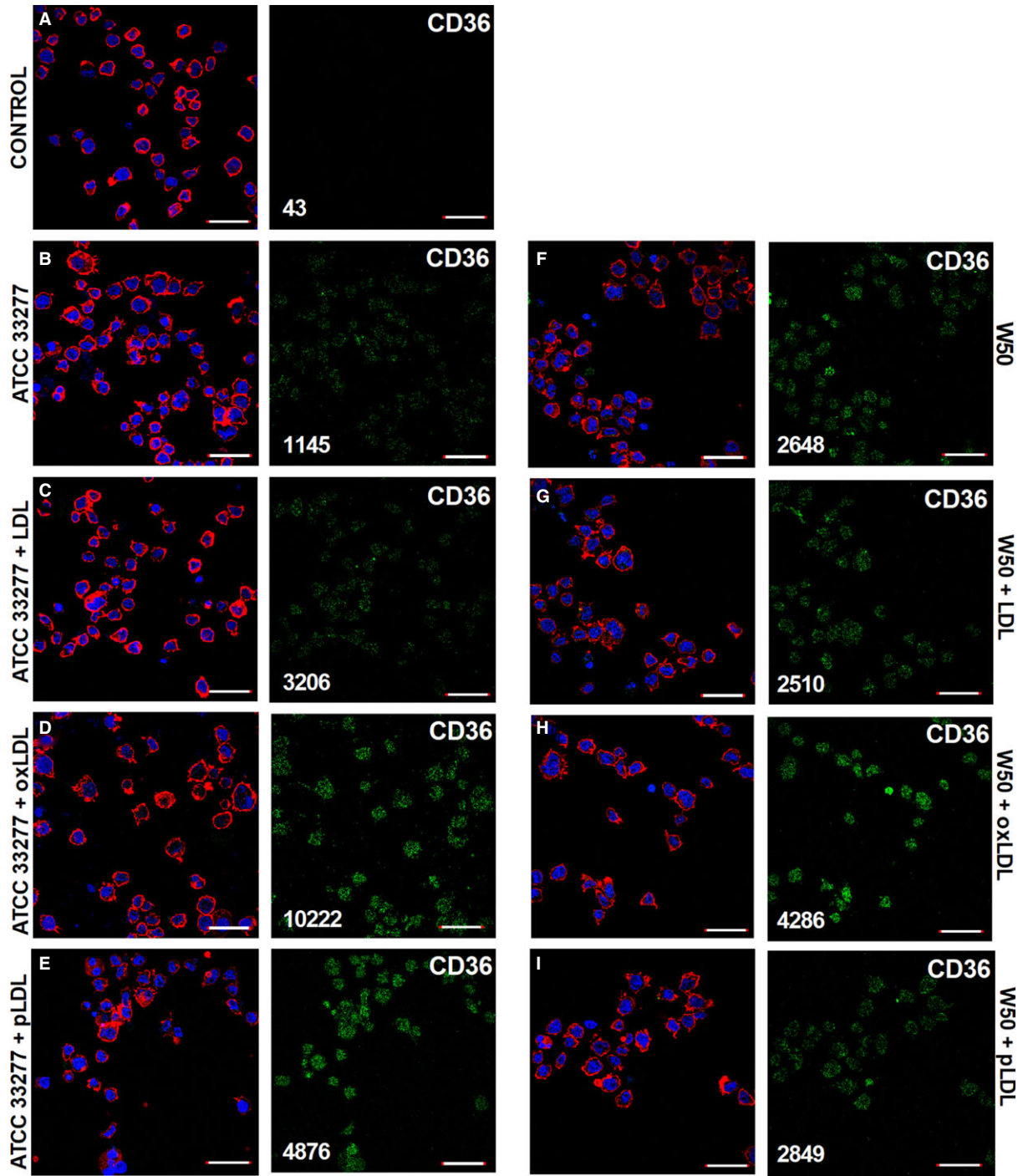


Fig. 5. The effects of *P. gingivalis* and LDL on CD36 expression on THP1 cells. THP1 cells were: Unstimulated (A) or stimulated with MOI100 *P. gingivalis* ATCC33277 (B–E) or W50 (F–I) and co-incubated without (B and F) or with 60 µg/mL of native LDL (C and G), oxLDL (D and H) or pLDL (E and I) for 6 h. FITC-labeled CD36 was added at 1:200 dilution and further stained for actin with Rhodamine phalloidin (red) and nucleus with DAPI (blue). Bar = 40 µm. 60× objective, oil immersion. Representative confocal images from three independent experiments are shown. The representative image for each condition was scanned and fluorescence was quantified using ImageJ and mean fluorescence intensity is indicated as numbers in the respective figures.

*P. gingivalis*-induced expression of CD36 in THP1 cells. These effects were most obvious with ATCC33277 compared to W50. Untreated THP1 cells did not show any expression of CD36. Co-incubation of *P. gingivalis* with oxLDL, resulted in a ~9-fold increase in mean fluorescence intensity in comparison to only ATCC33277, whereas, co-incubation with LDL and pLDL caused ~3- and 2-fold enhancement, respectively.

## DISCUSSION

In this study, we investigated the inflammatory responses of THP1 cells and how these responses were affected by native and modified LDL. A very thorough analysis of ROS production, caspase 1 activation, and IL-1 $\beta$  accumulation from 30 min up to 6 h was conducted. We found that ATCC33277 and W50 infection triggered ROS production, caspase 1 activation and release of IL-1 $\beta$  from THP1 cells. Oxidized LDL was capable of up-regulating CD36 expression and IL-1 $\beta$  secretion in THP1 cells. *Porphyromonas gingivalis* induced caspase 1 activation and IL-1 $\beta$  accumulation was altered in the presence of native and modified LDL.

Epidemiological analysis in humans and studies of murine models of atherosclerosis support a strong role for infectious agents like *P. gingivalis* in inflammatory atherosclerotic plaque accumulation (26). We have previously shown using proteomics that *P. gingivalis* modifies LDL in human blood, to an atherogenic form which supports a role of periodontal disease in the development of atherosclerosis (13). We have also demonstrated that patients with periodontitis exhibit altered immune response, leading to differential cytokine expression profiles, in saliva, GCF, and serum (27). A 30-min bacterial interaction with cells is of critical importance as Parahitayawa *et al.* have previously presented evidence of short, transient bacteremia with the highest intensity limited to the first 30 min after a trigger episode (28).

Phagocytic leukocytes such as neutrophils and monocytes, when appropriately stimulated, consume oxygen and produce ROS in a process often referred to as the respiratory burst. Furthermore, they secrete an array of proteolytic enzymes and pro-inflammatory cytokines. Also, NF- $\kappa$ B was the first eukaryotic transcription factor shown to respond directly to oxidative stress and NF- $\kappa$ B nuclear translocation has been suggested to directly involve in ROS production (13, 29–31). *Porphyromonas gingivalis*-generated ROS in THP1 cells exhibited a strain- and dose-dependent expression. Although ROS was expressed as early as 30 min

post-infection, it followed a gradual decline at higher MOI. In W50-infected cells, MOI 10 was optimal enough to induce a slow steady rise that was maintained over a longer period, suggesting a prolonged immune response. Hence, ROS is known to be able to cause oxidative damage to cells (31). Structural differences between *P. gingivalis* ATCC33277 and W50 could explain the delayed ROS induction by MOI 10 W50. The presence of an outer capsular layer and differences in fimbriae have, for instance, been seen to prevent bacterial uptake by phagocytes. As opposed to ATCC33277, W50 is sparsely fimbriated and possesses a capsule (32–34).

Previous studies have reported that RgpA/B and Kgp can induce secretion of pro-inflammatory cytokines like IL-1 $\beta$ , IL-6, CXCL8, MCP-1 from human monocytic cells via synergistic effects of PAR 1, 2, 3, toll-like receptors (TLR) 2, 4 and NOD1 and 2 (30, 35). Pro-IL-1 $\beta$  is generated by activation of TLRs and NF- $\kappa$ B (signal 1) and mature IL-1 $\beta$  is produced by inflammasome-dependent caspase 1 cleavage of pro-IL-1 $\beta$  (signal 2). TLRs are activated by *P. gingivalis* and its surface components such as LPS, lipoproteins, and fimbriae (35). We have shown that both *P. gingivalis* ATCC33277 and W50 induce in THP1 cells, a dose-dependent caspase 1 activity that gradually increased from 30 min reaching a peak at 2 h. We observed higher levels of IL-1 $\beta$  in the supernatants of MOI10 *P. gingivalis*-stimulated THP1 cells compared to MOI100. Our previous studies showed that the presence of functional gingipains hydrolyze CXCL8 in the supernatant of *P. gingivalis*-stimulated THP1 cells, and other studies have also indicated that IL-1 $\beta$  is vulnerable to hydrolysis by gingipains. Higher concentration of *P. gingivalis* could indicate the presence of more functional gingipains in the supernatant (36, 37).

We found that oxLDL appeared to act in synergy with MOI10 or MOI100 *P. gingivalis* ATCC33277 in augmenting IL-1 $\beta$  release from THP1 cells. The effect of *P. gingivalis* ATCC33277 pLDL, but not W50 pLDL on IL-1 $\beta$  release from THP1 cells was very intriguing. *Porphyromonas gingivalis* ATCC33277 pLDL at MOI1 and MOI10 induced significantly higher IL-1 $\beta$  release from THP1 cells compared to ATCC33277 alone. However, *P. gingivalis* ATCC33277 pLDL at MOI100 significantly down-regulated the IL-1 $\beta$  release, in respect to THP1 cells stimulated with ATCC33277 alone. In addition, at MOI100, co-incubation with pLDL resulted in lower IL-1 $\beta$  accumulation compared to co-incubation with native LDL. Caspase 1 analysis reflected the IL-1 $\beta$  picture by THP1 cells in respect to differences exhibited by both the strains of *P. gingivalis* and upon co-incubation with

native and modified LDL. We hypothesize that ATCC33277 at MOI100 can alter native LDL into a form that may suppress inflammasome activation. The results definitely confirm the need for more investigation as the above results seem to assert that strains, numbers, and the milieu could affect the outcome of chronic inflammatory process in both vascular and periodontal infection by *P. gingivalis*. This is of particular interest as the only difference between the native LDL and pLDL stimulations is that in pLDL, the native LDL was pre-incubated with the bacteria 30 min prior to stimulation. On co-incubating with native LDL, the bacteria and LDL come into contact only at the time of infecting THP1 cells. At this point, LDL is subjected to effects from bacteria, THP1 cells and by products of THP1 cells interaction with the bacteria. This has led us to speculate that in pLDL, the native LDL was already modified during the 30 min incubation with the bacteria and this modified product could have tangible regulatory effects on THP1 response to *P. gingivalis* ATCC33277.

LDL modification in vascular compartment may occur as a result of proteolytic effects of *P. gingivalis* and/or leukocyte proteases or by the oxidative burst response of phagocytes in the blood to *P. gingivalis* (38). LDL was reported to form aggregates with *P. gingivalis* and its outer membrane vesicles (OMV). This was associated with the degradation of the LDL apo B-100 protein (39). Hence, *P. gingivalis*-induced modification of LDL has to be further characterized and elucidated more in detail. In correlation, we have previously shown that *P. gingivalis* ATCC33277 modifies LDL in human blood *in vitro*, including Rgp-dependent cleavage of Apo B-100 (13). CD36 on monocytes and macrophages recognizes ligands of pathogens, such as *Streptococcus pneumoniae* and autologous agents like oxLDL and  $\beta$ -amyloid fibril. Ligation of these ligands will initiate both signals 1 and 2 for activation of the inflammasome, resulting in secretion of mature IL-1 $\beta$ . oxLDL and  $\beta$ -amyloid fibrils are key inflammatory components of atherosclerotic and Alzheimer plaques, respectively (22, 40). We showed that THP1 cells express CD36 in response to oxLDL, ATCC33277, W50, but not native LDL. Recognition of oxLDL by CD36 on monocytes could result in foam cell formation which is a forerunner of an atherosclerotic lesion (41). Similar to our findings regarding IL-1 $\beta$  release, *P. gingivalis* ATCC33277 exhibited a synergistic effect on CD36 expression on THP1 cells in the presence of oxLDL. However, W50 co-incubated with oxLDL induced a lower CD36 expression compared to oxLDL alone.

Studies in animal models have demonstrated that *P. gingivalis* strains vary in their virulence with

W50 classified as a virulent and ATCC33277 classified as an avirulent strain. Among the strains tested, ATCC33277 was reported to exhibit high proteolytic and moderate collagenolytic activity despite being one of the least infective strains (42, 43). This may serve to benefit survival of various strains of *P. gingivalis* in various niches and could also be used to diagnose the progression of periodontitis and associated systemic inflammatory diseases.

In conclusion, we observed that *P. gingivalis* induced inflammatory responses in a strain- and dose-dependent manner. Furthermore, ATCC33277 induced caspase 1 activation and IL-1 $\beta$  release was observed to be modified in the presence of native and modified LDL. Between the two bacterial strains tested, it is very evident that ATCC33277 responses underwent a more tangible modification in the presence of native and modified LDL comparison to W50. The pLDL responses were very interesting and hence, it is important that we explicate the mechanisms and the nature of *P. gingivalis*-mediated transformation of LDL protein structure and its effect on host cells. This would give us a closer insight into the pathogenesis of *P. gingivalis*-mediated inflammatory responses in monocytes.

---

The authors acknowledge the support from Swedish Heart and Lung Foundation, the Foundation of Olle Engkvist and the Knowledge Foundation. W50 was a kind gift from Dr. M. Curtis (Barts and The London, Queen Mary's School of Medicine and Dentistry, UK). We would like to thank Professor Jana Jass for the use of the confocal microscope for our research.

## CONFLICT OF INTEREST

The authors declare that they have no competing interests.

## REFERENCES

- Haynes WG, Stanford C. Periodontal disease and atherosclerosis: from dental to arterial plaque. *Arterioscler Thromb Vasc Biol* 2003;23:1309–11.
- Socransky SS, Haffajee AD, Cugini MA, Smith C, Kent RL Jr. Microbial complexes in subgingival plaque. *J Clin Periodontol* 1998;25:134–44.
- Kurita-Ochiai T, Yamamoto M. Periodontal pathogens and atherosclerosis: implications of inflammation and oxidative modification of LDL. *Biomed Res Int* 2014;2014:595981.
- Guo Y, Nguyen KA, Potempa J. Dichotomy of gingipains action as virulence factors: from cleaving substrates with the precision of a surgeon's knife to a

- meat chopper-like brutal degradation of proteins. *Periodontology* 2000;2010:15–44.
5. Bartova J, Sommerova P, Lyuya-Mi Y, Mysak J, Prochazkova J, Duskova J, et al. Periodontitis as a risk factor of atherosclerosis. *J Immunol Res* 2014;2014:636893.
  6. Janket SJ, Baird AE, Chuang SK, Jones JA. Meta-analysis of periodontal disease and risk of coronary heart disease and stroke. *Oral Surg Oral Med Oral Pathol Oral Radiol Endod* 2003;95:559–69.
  7. Humphrey LL, Fu R, Buckley DI, Freeman M, Helfand M. Periodontal disease and coronary heart disease incidence: a systematic review and meta-analysis. *J Gen Intern Med* 2008;23:2079–86.
  8. Beck JD, Offenbacher S. The association between periodontal diseases and cardiovascular diseases: a state-of-the-science review. *Ann Periodontol* 2001;6:9–15.
  9. Orlova EV, Sherman MB, Chiu W, Mowri H, Smith LC, Gotto AM Jr. Three-dimensional structure of low density lipoproteins by electron cryomicroscopy. *Proc Natl Acad Sci USA* 1999;96:8420–5.
  10. Khovidhunkit W, Kim MS, Memon RA, Shigenaga JK, Moser AH, Feingold KR, et al. Effects of infection and inflammation on lipid and lipoprotein metabolism: mechanisms and consequences to the host. *J Lipid Res* 2004;45:1169–96.
  11. Feingold KR, Grunfeld C. The effect of inflammation and infection on lipids and lipoproteins. In: De Groot LJ, Beck-Peccoz P, Chrousos G, Dungan K, Grossman A, Hershman JM, Koch C, McLachlan R, New M, Rebar R, Singer F, Vinik A, Weickert MO, editors. *Endotext*. South Dartmouth (MA): MDText.com, Inc, 2000.
  12. Pussinen PJ, Vilkkuna-Rautiainen T, Alftan G, Palo-suo T, Jauhiainen M, Sundvall J, et al. Severe periodontitis enhances macrophage activation via increased serum lipopolysaccharide. *Arterioscler Thromb Vasc Biol* 2004;24:2174–80.
  13. Bengtsson T, Karlsson H, Gunnarsson P, Skoglund C, Elison C, Leanderson P, et al. The periodontal pathogen *Porphyromonas gingivalis* cleaves apoB-100 and increases the expression of apoM in LDL in whole blood leading to cell proliferation. *J Intern Med* 2008;263:558–71.
  14. Grenier D, La VD. Proteases of *Porphyromonas gingivalis* as important virulence factors in periodontal disease and potential targets for plant-derived compounds: a review article. *Curr Drug Targets* 2011;12:322–31.
  15. Qi M, Miyakawa H, Kuramitsu HK. *Porphyromonas gingivalis* induces murine macrophage foam cell formation. *Microb Pathog* 2003;35:259–67.
  16. Salvayre R, Auge N, Benoist H, Negre-Salvayre A. Oxidized low-density lipoprotein-induced apoptosis. *Biochem Biophys Acta* 2002;1585:213–21.
  17. Yazgan B, Ustunsoy S, Karademir B, Kartal-Ozer N. CD36 as a biomarker of atherosclerosis. *Free Radic Biol Med* 2014;75(Suppl 1):S10.
  18. Silverstein RL, Febbraio M. CD36, a scavenger receptor involved in immunity, metabolism, angiogenesis, and behavior. *Sci Signal* 2009;2:re3.
  19. Brown PM, Kennedy DJ, Morton RE, Febbraio M. CD36/SR-B2-TLR2 dependent pathways enhance *Porphyromonas gingivalis* mediated atherosclerosis in the Ldlr KO mouse model. *PLoS ONE* 2015;10:e0125126.
  20. Stewart CR, Stuart LM, Wilkinson K, van Gils JM, Deng J, Halle A, et al. CD36 ligands promote sterile inflammation through assembly of a Toll-like receptor 4 and 6 heterodimer. *Nat Immunol* 2010;11:155–61.
  21. Park YM. CD36, a scavenger receptor implicated in atherosclerosis. *Exp Mol Med* 2014;46:e99.
  22. Sheedy FJ, Grebe A, Rayner KJ, Kalantari P, Ramkhalawon B, Carpenter SB, et al. CD36 coordinates NLRP3 inflammasome activation by facilitating intracellular nucleation of soluble ligands into particulate ligands in sterile inflammation. *Nat Immunol* 2013;14:812–20.
  23. Yin Y, Pastrana JL, Li X, Huang X, Mallilankaraman K, Choi ET, et al. Inflammasomes: sensors of metabolic stresses for vascular inflammation. *Front Biosci* 2013;18:638–49.
  24. Xu L, Dai Perrard X, Perrard JL, Yang D, Xiao X, Teng BB, et al. Foamy monocytes form early and contribute to nascent atherosclerosis in mice with hypercholesterolemia. *Arterioscler Thromb Vasc Biol* 2015;35:1787–97.
  25. Jensen EC. Quantitative analysis of histological staining and fluorescence using ImageJ. *Anat Rec* 2013;296:378–81.
  26. Hayashi C, Viereck J, Hua N, Phinikaridou A, Madrigal AG, Gibson FC 3rd, et al. *Porphyromonas gingivalis* accelerates inflammatory atherosclerosis in the innominate artery of ApoE deficient mice. *Atherosclerosis* 2011;215:52–9.
  27. Khalaf H, Lonn J, Bengtsson T. Cytokines and chemokines are differentially expressed in patients with periodontitis: possible role for TGF-beta1 as a marker for disease progression. *Cytokine* 2014;67:29–35.
  28. Parahitiyawa NB, Jin LJ, Leung WK, Yam WC, Samaranyake LP. Microbiology of odontogenic bacteremia: beyond endocarditis. *Clin Microbiol Rev* 2009;22:46–64.
  29. Robinson JM. Reactive oxygen species in phagocytic leukocytes. *Histochem Cell Biol* 2008;130:281–97.
  30. Uehara A, Imamura T, Potempa J, Travis J, Takada H. Gingipains from *Porphyromonas gingivalis* synergistically induce the production of proinflammatory cytokines through protease-activated receptors with Toll-like receptor and NOD1/2 ligands in human monocytic cells. *Cell Microbiol* 2008;10:1181–9.
  31. Kunsch C, Medford RM. Oxidative stress as a regulator of gene expression in the vasculature. *Circ Res* 1999;85:753–66.
  32. Kato T, Kawai S, Nakano K, Inaba H, Kuboniwa M, Nakagawa I, et al. Virulence of *Porphyromonas gingivalis* is altered by substitution of fimbria gene with different genotype. *Cell Microbiol* 2007;9:753–65.
  33. Tachibana-Ono M, Yoshida A, Kataoka S, Ansai T, Shintani Y, Takahashi Y, et al. Identification of the genes associated with a virulent strain of *Porphyromonas gingivalis* using the subtractive hybridization technique. *Oral Microbiol Immunol* 2008;23:84–7.
  34. Singh A, Wyant T, Anaya-Bergman C, Aduse-Opoku J, Brunner J, Laine ML, et al. The capsule of *Porphyromonas gingivalis* leads to a reduction in the host

- inflammatory response, evasion of phagocytosis, and increase in virulence. *Infect Immun* 2011;79:4533–42.
35. Park E, Na HS, Song YR, Shin SY, Kim YM, Chung J. Activation of NLRP3 and AIM2 inflammasomes by *Porphyromonas gingivalis* infection. *Infect Immun* 2014;82:112–23.
  36. Jayaprakash K, Khalaf H, Bengtsson T. Gingipains from *Porphyromonas gingivalis* play a significant role in induction and regulation of CXCL8 in THP-1 cells. *BMC Microbiol* 2014;14:193.
  37. Stathopoulou PG, Benakanakere MR, Galicia JC, Kinane DF. The host cytokine response to *Porphyromonas gingivalis* is modified by gingipains. *Oral Microbiol Immunol* 2009;24:11–7.
  38. Lönn J, Ljunggren S, Klarström-Engström K, Demirel I, Bengtsson T, Karlsson H. Lipoprotein modifications by gingipains of *Porphyromonas gingivalis*. *J Periodontol Res* 2018;53:403–13.
  39. Miyakawa H, Honma K, Qi M, Kuramitsu HK. Interaction of *Porphyromonas gingivalis* with low-density lipoproteins: implications for a role for periodontitis in atherosclerosis. *J Periodontol Res* 2004;39:1–9.
  40. Binder CJ, Hökkö S, Dewan A, Chang MK, Kieu EP, Goodyear CS, et al. Pneumococcal vaccination decreases atherosclerotic lesion formation: molecular mimicry between *Streptococcus pneumoniae* and oxidized LDL. *Nat Med* 2003;9:736–43.
  41. Yu XH, Fu YC, Zhang DW, Yin K, Tang CK. Foam cells in atherosclerosis. *Clin Chim Acta* 2013;424:245–52.
  42. Grenier D, Mayrand D. Selected characteristics of pathogenic and nonpathogenic strains of *Bacteroides gingivalis*. *J Clin Microbiol* 1987;25:738–40.
  43. Chen T, Hosogi Y, Nishikawa K, Abbey K, Fleischmann RD, Walling J, et al. Comparative whole-genome analysis of virulent and avirulent strains of *Porphyromonas gingivalis*. *J Bacteriol* 2004;186:5473–9.